ACS OMEGA

Open Access

http://pubs.acs.org/journal/acsodf

Article

Sensors Based on Tin and Indium Oxides for the Determination of Acetone in Human Breath

Tatiana Kimakova, Daria Kondrakhova, Evgeni Ovodok, Marya Ivanovskaya, Valentina Kormosh, Serhii Vorobiov, Maksym Lisnichuk, Vitalij Bilanych, and Vladimir Komanicky*

Cite This: *ACS Omega* 2023, 8, 40078−40086

Read Online

ACCESS | Metrics & More | Article Recommendations

ABSTRACT: The properties of planar sensors based on tin dioxide and indium oxide used for the determination of acetone vapors have been studied. Sensors based on synthesized SnO_2 and In_2O_3 nanopowders showed high sensitivity to low concentrations of acetone in a humid environment which simulates human exhalation. The addition of a small amount of Au^{III} ions to hydroxide sols significantly increases the threshold sensitivity and the sensor response in a wide range of acetone concentrations. In_2O_3−Au sensors have the maximum sensitivity at an operating temperature of 325 °C. The In_2O_3−Au-sensors reliably record the change in acetone concentration in the concentration range from a minimum of 0.1 to 5 ppm with high accuracy, which is necessary for rapid diagnostics of the condition of patients with diabetes (1.8−5.0 ppm). The high sensitivity of the obtained sensors is explained by the structural features and the surface conditions of oxides and gold nanoparticles, which depend on the sample synthesis conditions.

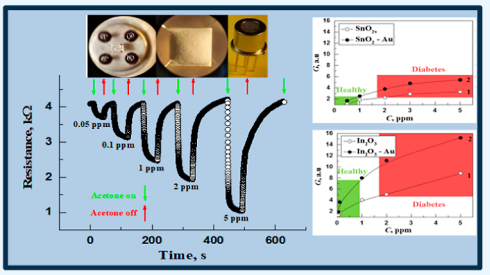

INTRODUCTION

Methods to identify disease markers are used to diagnose various diseases and monitor the health status of chronically ill patients.[1,2] In particular, the possibilities of determining certain substances in human exhalation in dental diseases and diabetes are being widely studied.[3,4] Many of these substances are present in the exhalation of a healthy person, but their concentration increases significantly in the presence of a disease. The main research in this area is aimed at identifying acetone in human exhalation as a biomarker for diabetes since the concentration of other substances is much lower. Along with the most common method of chromatography, intensive work has been carried out in recent years that is aimed at establishing the possibility of determining acetone using sensors. Cheaper and faster approaches are being sought to control the content of various substances in exhaled air because carrying out chromatographic analysis is quite laborious. The use of semiconductor gas sensors[4,5] or self-powered sensors based on triboelectric nanogenerator[6−9] for primary express analysis of acetone concentration are the variants of one of these approaches. Human exhalation analysis is a painless diagnostic method that can complement classical diagnostic methods.

Currently, commercial sensors for volatile organic substances, including acetone, are produced.[5] However, these sensors are designed to detect high concentrations of acetone (5−500 ppm). It should be noted that it is impossible to achieve selectivity in the analysis of volatile organic substances on resistive sensors based on metal oxides since the mechanism of their detection is similar. Therefore, it is necessary to use multisensor systems with cross-reacting sensors with a signal recognition system of the "electronic nose" type when analyzing complex gas mixtures.[10,11]

It was found that the acetone concentration in exhaled breath of healthy people ranges between 0.3 and 0.9 ppm.[12] Sensors with high sensitivity to low concentrations of acetone (0.9−3 ppm) in a humid environment are needed for monitoring and diagnosing diabetes. The search for promising materials for such sensors has been intensively carried out. Huge experimental work has been carried out to test various metal oxide materials as acetone sensors and the results of the studies are summarized in reviews.[5,12] SnO_2, In_2O_3, CuO, WO_3, TiO_2 oxides, etc., are used as semiconductor oxides in gas sensors.[5,12−16] An analysis of the available data shows that it is possible to identify directions for increasing the sensitivity of metal oxide sensors to acetone. Two approaches can be distinguished:

1. Improving the synthesis technology to obtain nanosized metal oxides with an active surface for adsorption and catalysis.

Received: March 30, 2023
Accepted: September 15, 2023
Published: October 18, 2023

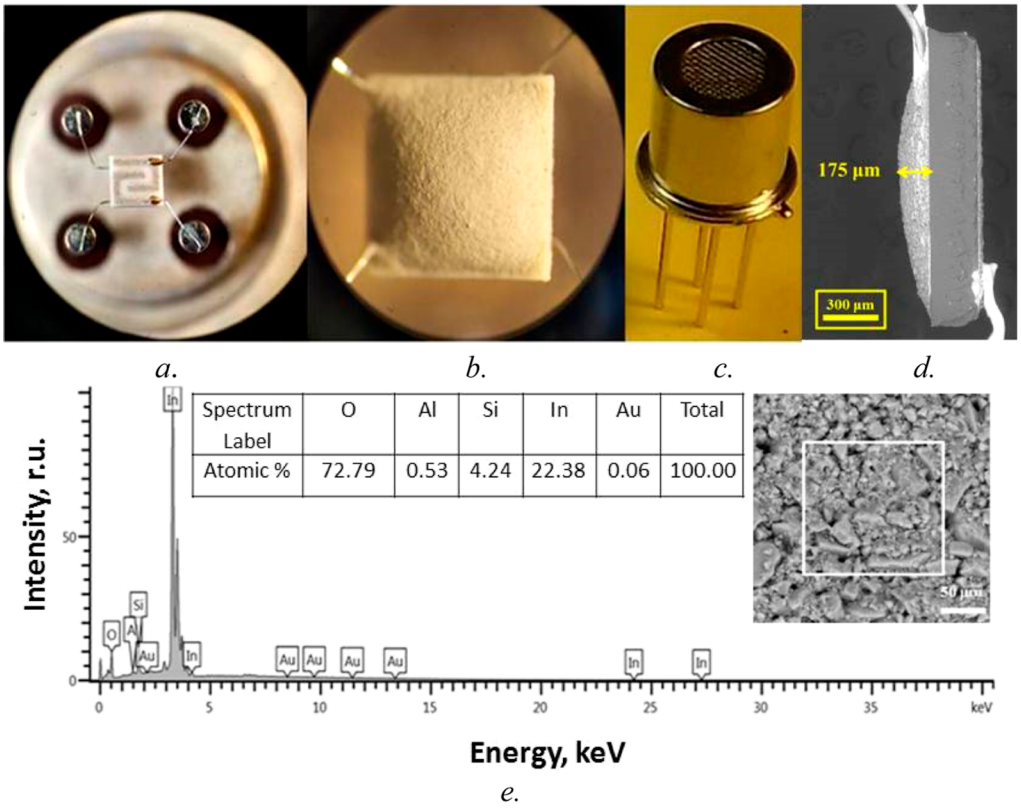

Figure 1. Appearance of the platform with measuring electrodes (a), the platform with the applied gas-sensitive film (b), the finished gas sensor (c), SEM image of the platform with the film (d), and In_2O_3−Au film EDAX (e).

2. The injection of activating additives and, primarily, catalytically active metals.

Both approaches were implemented in this work. We present the development of planar-type sensors on the standard microheating platforms with sensitivity to acetone in the concentration range of 1−5 ppm. To create acetone sensors, SnO_2 and In_2O_3, which are widely used materials in the production of gas sensors, were utilized. The use of SnO_2 and In_2O_3 as gas sensors is due to their chemical stability and semiconductor properties, as well as a wide band gap.

SUBSTANTIATION OF METHODS FOR THE SYNTHESIS OF MATERIALS

Tin dioxide is the most widely used material in the manufacture of gas sensors for toxic and combustible gases. The advantages of SnO_2 are high thermal and chemical stability and excellent electrical properties, in particular a wide band gap of 3.6 eV. Its application fits into the existing machine technology for manufacturing sensors. The sensitivity of SnO_2 is low in a clean state, but with the introduction of activating additives, the sensitivity can be significantly increased.[5,12,17]

To fabricate sensors, we synthesized SnO_2 from either $SnCl_4$ or $SnCl_2$. However, the negative effect of the presence of chloride ions on the adsorption-catalytic properties of the oxide is known. This explains the insufficiently high sensitivity of the SnO_2 sensors to CO and CH_4. The use of other tin salts makes it possible to eliminate the negative effect of chloride ion impurities on the adsorption and catalytic properties of SnO_2. The modulating effect of sulfate ions on the surface state of various metal oxides is known, which favorably affects their catalytic properties in oxidation reactions.[18−20] We developed an original technology for the synthesis of tin dioxide from $SnSO_4$ taking into account these data. Our synthesis technology not only eliminates chloride ions in the precursors but also leads to the production of an ultrafine SnO_2 powder with a surface that is modified by sulfate groups.[18−20]

It was shown earlier that indium oxide is more sensitive to many gases compared to tin dioxide, but it is less chemically and thermally stable.[17] Indium oxide is a very promising material for thin-film sensors, where its good film-forming properties and high electrical conductivity are important qualities.[21]

We used Au as a catalyst instead of the Pd activator, which is traditionally used in the production of gas sensors. It is known that bulk Au is inert and does not exhibit a catalytic activity.

It was found that gold catalyzes various redox reactions when the size of gold particles is reduced to nanosize.[22] The problem is obtaining nanosized gold particles after the samples. The use of the sol−gel technique for obtaining oxide systems with the introduction of $HAuCl_4$ into the sol during the synthesis is a feature of the approach in this work.[23] The sol−gel procedures used in this work for the synthesis of oxide systems make it possible to insert gold ions into hydrosols. This allowed us to provide the stabilization of the nanosized state of gold in the resulting MeO_x−Au system upon heating.[23,24] In addition, such an insertion technique of gold favors the formation of an active MeO_x−Au interface in adsorption and catalysis.[17,23−26]

SYNTHESIS TECHNOLOGY

Tin dioxide was synthesized according to a previously developed procedure, which makes it possible to obtain

https://doi.org/10.1021/acsomega.3c02125
ACS Omega 2023, 8, 40078−40086

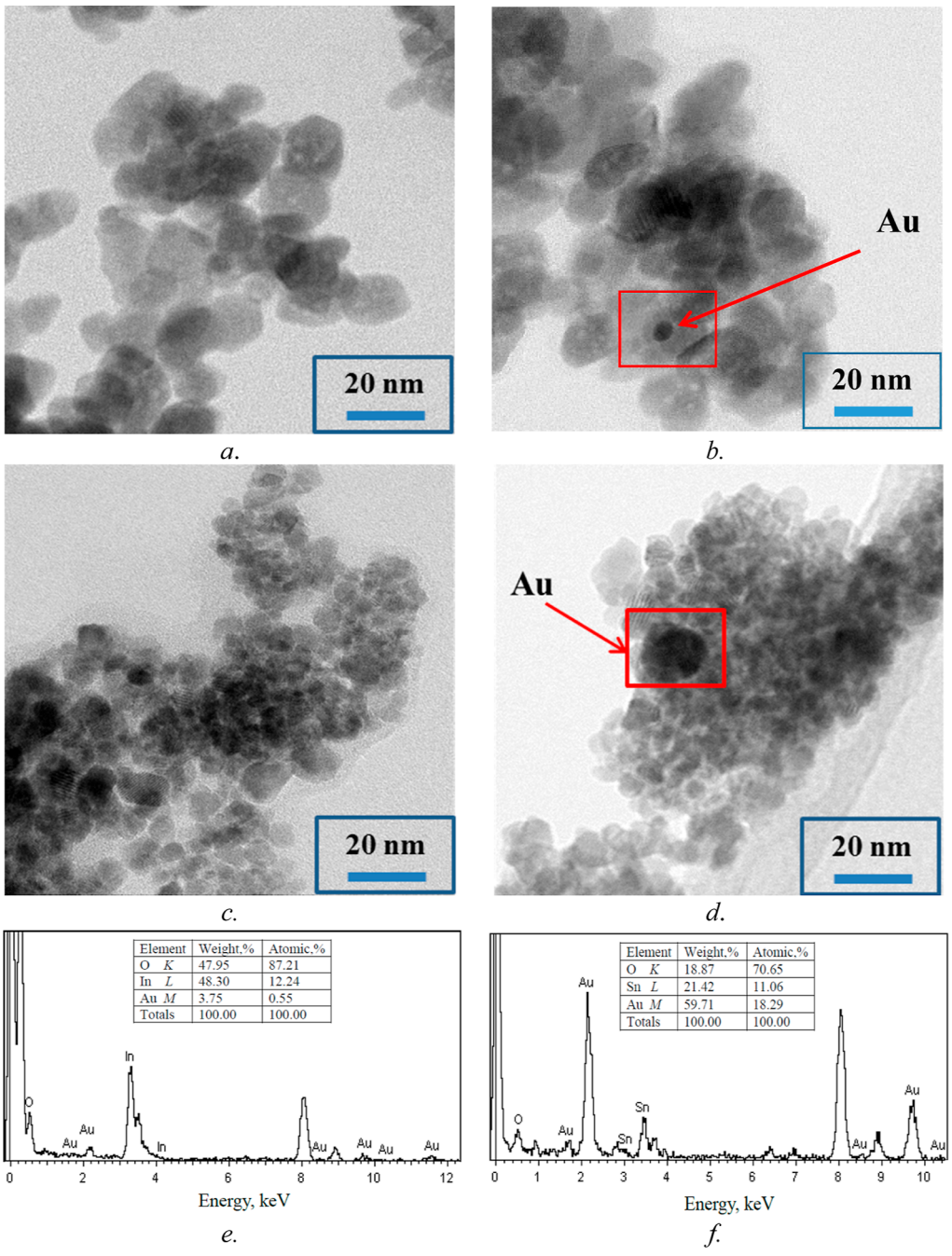

Figure 2. TEM images of In_2O_3 (a), In_2O_3–Au (b), SnO_2 (c), and SnO_2–Au (d) powders and EDAX spectrum of In_2O_3–Au (e) and SnO_2–Au (f) powders.

small tin dioxide particles with surface modification by sulfate groups.[18] The synthesis procedure includes pretreatment of $SnSO_4$ by heating in H_2SO_4 followed by the preparation of $SnO_2{\cdot}nH_2O$ sols by the standard method and their transformation into powder by drying at 50 °C and heating in air at 600 °C.

Indium oxide was synthesized by the sol–gel method from $In(NO_3)_3$ using NH_4OH according to the previously published procedure with sol stabilization with nitric acid.[23] In_2O_3 powder was obtained by heating the xerogel of indium hydroxide at 600 °C.

The solution of $HAuCl_4$ was introduced into the sol of SnO_2 nH_2O and $In(OH)_3$ in an amount of 0.2 wt % Au relative to oxide to obtain SnO_2–Au and In_2O_3–Au nanocomposites. Then, the sols with the addition of Au^{III} were dried and heated at 600 °C.

The X-ray diffraction (XRD) measurements were performed by using a Philips X-ray PANalytical Empyrean diffractometer with Cu Kα radiation. The particle size was estimated on a transmission electron microscope. Scanning transmission electron microscopy images were acquired by JEOL 2100F at an accelerating voltage of 200 kV.

MANUFACTURING OF SENSORS

The sensors were fabricated by using thick film technology. An aluminosilicate suspension (semicolloidal solution of silicic acid and aluminum nitrate) was added to the powders (In_2O_3, In_2O_3–Au, SnO_2, SnO_2–Au) and thoroughly dispersed. As a

https://doi.org/10.1021/acsomega.3c02125
ACS Omega 2023, 8, 40078–40086

result, a mixture was obtained that was applied with a microdoser to the sensor microplatforms from the side of the measuring electrodes. We used standard microplatforms made of aluminum oxide substrates 1.6 × 1.6 × 0.3 mm^3 in size with a platinum heater and measuring electrodes. The appearance of sensor elements is given in Figure 1. Heat resistance at room temperature was 16 ± 1 Ω. Furthermore, the process of drying and annealing (baking) was carried out at 600 °C. The aluminosilicate suspension formed a porous carcass during annealing, which contained powders of gas-sensitive materials. Thus, a solid porous gas-sensitive film was formed as a result of sintering (Figure 1b). The film thickness in the center was 175 μm. The film thickness was thinner at the edges of the platform compared to that of the central part (Figure 1d).

Al and Si atoms of the aluminosilicate carcass were in the EDAX spectrum of the sensor film in addition to the atoms (In, O, and Au) of the initial powders (Figure 1e).

The sensitive elements were fixed in standard housings (Figure 1c). The resistance of the sensors was measured under static voltage conditions in air (R_0) and in acetone-air mixtures (R_g) with a relative humidity of 98%. The output signals (G) of the sensors were determined as the ratio of resistances: $G = R_0/R_g$. The response time (T_{Res}) of the sensors was determined as the time to reach 90% of the output signal. The recovery time (T_{Rec}) was defined as the time to reverse the change in 90% of the output signal after the cessation of exposure to acetone vapor.

It is known that the concentration of acetone in the air exhaled by a person is on an average of $10^{-6} - 10^{-7}$ mg/cm^3.[27] It is generally accepted that the concentration of acetone in exhaled air is less than 0.9 ppm in healthy humans. In a person with diabetes, the concentration of acetone in his exhalation exceeds 1.8 ppm.[28,29] For acetone, 1 ppm = 2.54 mg/m^3.[27] We prepared vapors of acetone with concentrations of 0.1, 0.5, 1, 2, 3, 5, and 50 ppm in equilibrium with a solution of acetone in distilled water according to the procedure described.[27,30]

We used an aqueous solution of acetone with a concentration of ∼10^{-4} mg/cm^3 to obtain the desired concentrations of the equilibrium vapor of acetone in a closed vessel and used the Henry coefficient for this level of concentrations of aqueous acetone solutions.[31] We also took into account the temperature dependence of K given.[31] Air humidity can affect the accuracy of gas detection, including that of acetone vapor. Usually, an increase in humidity worsens the adsorption-sensitive characteristics of the sensors. It is known that the relative humidity of human exhalation air can vary within fairly wide limits. However, it is less than the humidity of saturated water vapor in a closed vessel (100%). For example, the relative humidity of the human exhalation air is in the range of 41.9−91.0% according to the data given.[32] Gas sensors (connected by conductors to the measuring system) were introduced into a closed vessel with acetone vapors of appropriate concentrations for measurements. The vessel with the sensor was also hermetically sealed during measurements.

RESULTS AND DISCUSSION

Dispersion and Structural Features of Samples. Figure 2 shows TEM images of SnO_2 and In_2O_3 powders. The presented TEM images show that the synthesized oxide powders consist of nanosized particles. The diameter of SnO_2 particles is 4−6 nm (d_{av} ≈ 5.5 nm). The In_2O_3 particles are larger and have a rounded shape with an average diameter of 18−20 nm. The average particle diameter in In_2O_3−Au is slightly smaller, 14−16 nm.

Only one rutile-type crystalline phase is identified by XRD in the synthesized SnO_2 sample after heating at 600 °C (JCPDS 41−1445) (Figure 3). The SnO_2 reflections are broadened.

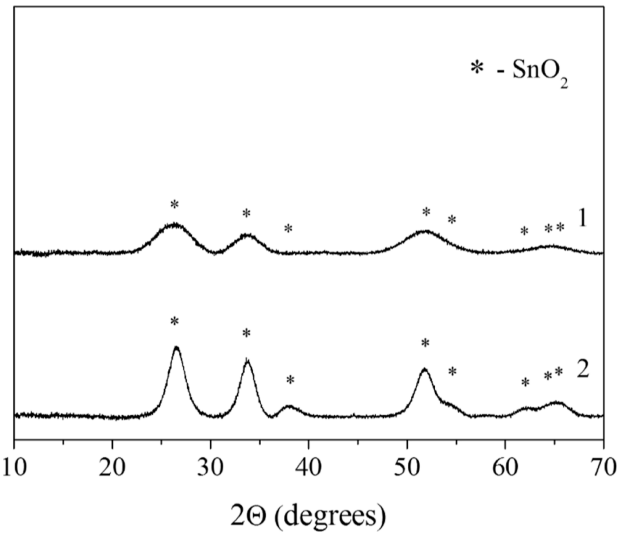

Figure 3. XRD patterns of the SnO_2 samples after heating at different temperatures: 1−50 °C and 2−600 °C.

The calculated coherent scattering region value is about 5 nm, and this agrees with the TEM data. The unit cell parameters of SnO_2 correspond to reference data (a = 0.4738 nm, and c = 0.3187 nm).

The presence of the Sn^{2+} impurity in such a sample as well as the presence of S in the form of SO_4^{2-} were previously established by the XPS method.[24] The stabilization of sulfate groups on the SnO_2 surface was also confirmed by IR spectroscopy.[24,26]

XRD patterns of In_2O_3 and In_2O_3−Au samples at different heating temperatures are shown in Figure 4. The cubic phase C-In_2O_3 (JCPDS 22−0336) is the main product during the thermal dehydration of the $In(OH)_3$ sol. The process of formation of the crystal structure of In_2O_3 (without and with the addition of Au^{III}) occurs with the formation of an impurity of the metastable hexagonal phase H-In_2O_3 (JCPDS 06-0416) at 300−500 °C that transforms into the thermally stable cubic phase of C-In_2O_3 after 600 °C. This process of structure formation promotes the formation of C-In_2O_3 with a deviation from oxygen stoichiometry.[33] C-In_2O_3 is characterized by defects in the form of oxygen vacancies and In^{2+} ions. The high conductivity of In_2O_3 is due to the presence of oxygen vacancies (F centers), In^+ and In^{2+} ions, and the ease of electron exchange between them.[34] In indium oxide, a band mechanism of electron transfer is assumed as a result of overlapping levels of In^+ and In^{3+}.

The crystallization process slows down slightly in the presence of gold. As a result, the sizes of In_2O_3 particles decrease and the content of hydroxyl groups on the surface increases.[23] Metallic gold was not detected in the SnO_2−Au and In_2O_3−Au samples by XRD due to the low Au concentration. Usually, highly dispersed gold is fixed on the surface of oxides by a (111) plane. Highly dispersed gold has a thin hemispherical shape at small sizes.[35] Au can form small clusters comprising only several atoms due to the small gold

https://doi.org/10.1021/acsomega.3c02125
ACS Omega 2023, 8, 40078−40086

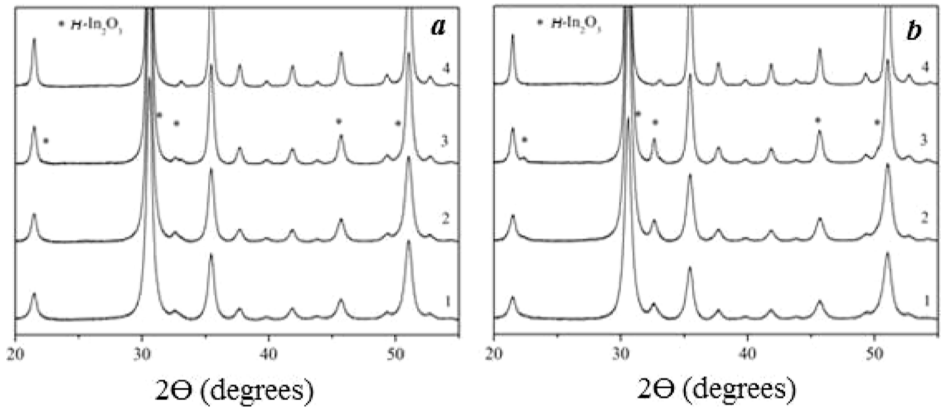

Figure 4. XRD patterns of In_2O_3 and In_2O_3–Au samples heated at different temperatures: 1–300, 2–400, 3–500, and 4–600 °C.

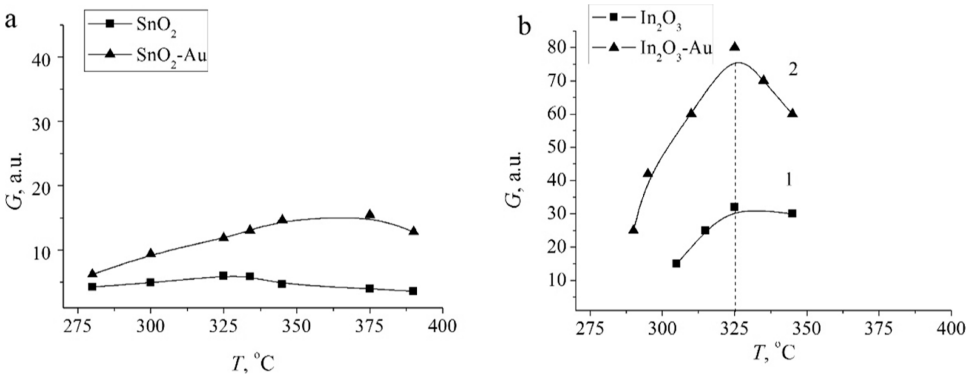

Figure 5. Dependence of the output signal (G) of the sensors on the operating temperature at 50 ppm acetone in a humid atmosphere: a—SnO_2 (1); SnO_2–Au (2); b—In_2O_3 (1); In_2O_3–Au (2).

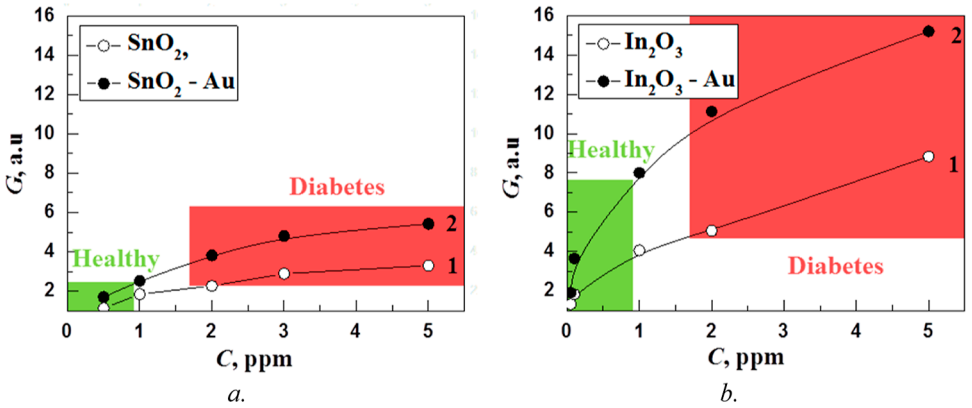

Figure 6. Dependences of the output signals (G) of the sensors on the concentration of acetone at the optimal detection temperature: a—SnO_2 (1), SnO_2–Au (2); b—In_2O_3 (1); In_2O_3–Au (2).

content, which is difficult to observe on the electron microscope.[36]

Au nanoparticles were detected in the synthesized In_2O_3–Au (Figure 2b) and SnO_2–Au (Figure 2d) powders by the scanning transmission electron microscopy method. The detected Au particles in these powders were about 5 and 12 nm in size, respectively. Au nanoparticles are shown in red rectangles. The Au atoms in these nanoparticles were confirmed by measurements of the EDAX spectra (Figure 2e,f).

The presence of Au^0 in the synthesized SnO_2–Au and In_2O_3–Au samples was confirmed by optical spectroscopy[37] and in SnO_2–Au by the XPS method.[24]

Properties of Sensors in the Determination of Acetone Vapors. Figure 5 shows the dependence of the output signals of the sensors on the operating temperature at 50 ppm of acetone in a humid atmosphere. The presented dependences make it possible to establish the optimal operating temperature for the detection of acetone on sensors with different chemical compositions of the sensitive elements. A strong increase in the sensor response was found when gold was added to the starting material. This is a special characteristic of indium oxide. The output signal also increases in the case of SnO_2–Au, but its value is lower than that for In_2O_3-sensors without the addition of gold. The optimum

https://doi.org/10.1021/acsomega.3c02125
ACS Omega 2023, 8, 40078–40086

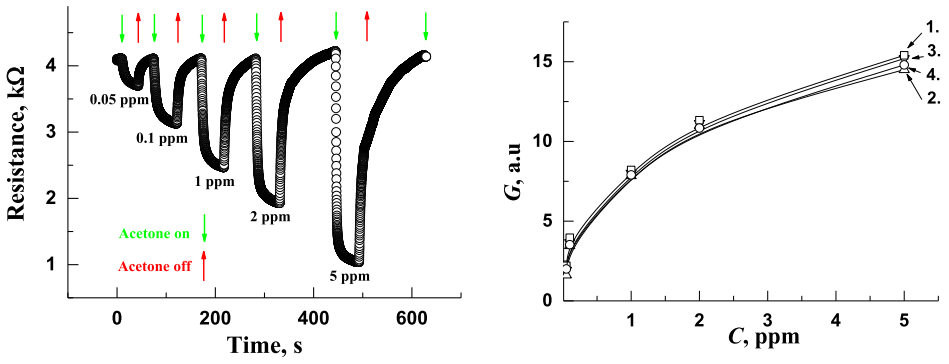

a. b.

Figure 7. Dynamics of the In_2O_3-Au sensor signal changes during detection of different concentrations of acetone in an adsorption−desorption cycle (a). Acetone on: the sensor is in a closed vessel with acetone vapor. Acetone off: the sensor is in air without acetone vapors. Change in the output signals of the In_2O_3−Au sensor during the detection of acetone (b). Curve 1.—after 2 days of storage of the sensor at room temperature, 2.—after 4 days of storage, 3.—after 6 days of storage, 4—after 1.

Table 1. Comparison of the Parameters of Sensors In_2O_3 and In_2O_3−Au Presented in This Study with Sensors Known from the Literature

composition	structure, morphology	*C*, ppm, acetone	output signal, *G*	*T*, °C	source
In_2O_3	mesoporous particles	50	29.8	300	38
In_2O_3−Sb	thin film	80	20	300	39
In_2O_3/Pd	nanoparticles	100	30.6	370	40
In_2O_3/Pt	rods/nanoparticles	1	6.2	320	41
In_2O_3	nanoparticles	50	11.6	240	42
In_2O_3/Au	hybrid structures	50	10.2	240	39
In_2O_3	hollow spheres	100	8	300	40
In_2O_3	nanospheres	30	11	200	43
In_2O_3	nanowire	100	4.2	400	44
In_2O_3	mesostructures	100	13.5	220	45
In_2O_3	nanoparticles	50	32	325	this work
		1	3.3		
		C_{lim} = 0.04			
In_2O_3−Au	nanoparticles	50	80	325	this work
		1	8		
		C_{lim} = 0.02			

acetone detection temperature for In_2O_3−Au sensors is lower (325 °C) than that for SnO_2−Au sensors (360 °C).

Figure 6 shows the dependence of the output signals of the sensors on the concentration of acetone at the optimal detection temperature. Sensors based on synthesized SnO_2 and In_2O_3 show a high sensitivity to low concentrations of acetone in a humid atmosphere. In_2O_3−Au-sensors have the highest threshold sensitivity (C_{lim} = 0.02 ppm). In_2O_3 sensors (C_{lim} = 0.04 ppm) are 10 times more sensitive than SnO_2 sensors (C_{lim} = 0.4 ppm) in terms of the minimum detectable acetone concentration.

Obtained concentration dependences reflect a significant change in the response of sensors, especially In_2O_3−Au, to low acetone concentrations in the range from C_{lim} to 5 ppm. This is important for reliable registration of small changes in the acetone concentration in exhalation during express diagnostics. The concentration of acetone in the exhalation of a healthy person can be up to 0.9 ppm.[3,4,12] The threshold concentration is 1.8 ppm for the diagnosis of diabetes, and it can increase to 3 ppm depending on the disease severity. The output signals of the sensors increase in the following order SnO_2 < SnO_2−Au < In_2O_3 < In_2O_3−Au in the concentration range from C_{lim} to 5 ppm.

It can be seen from the figure that a reliable fixation of the sensor signal is observed over the entire presented range of concentrations (including the range of concentrations of acetone in the exhalation of healthy people). The sensor recovery (desorption) time increases from 30 to 130 s if the acetone concentration changes from 0.05 to 5 ppm when the sensor is exposed to acetone vapor (absorption) for 40 s. Obviously, the time between measurements should be greater than the maximum desorption time when using such a sensor in a device for diagnosing diabetes. The sensor readings are well produced within 10 days of storing the sensors at room temperature and when warming the sensors at 100° above operating temperature before measuring the output signals during acetone detection (Figure 7 b). There is no stability degradation of the sensors over 10 days.

We compared the parameters of the In_2O_3 and In_2O_3−Au sensors developed by us with analogues known from the literature. The parameters of the sensors are shown in Table 1.

It follows from the presented data that the In_2O_3 sol−gel synthesized in the form of isotropic nanoparticles with a diameter of 18−20 nm is superior in sensitivity to the In_2O_3 samples with different particle morphologies which are described in the literature. Sensors based on the In_2O_3−Au

https://doi.org/10.1021/acsomega.3c02125
ACS Omega 2023, 8, 40078−40086

composite which are obtained by the method of inserting gold ions into an indium hydroxide sol also outperform sensors based on indium oxide with deposited metals In_2O_3−Pd and In_2O_3−Au in terms of the output signal.[39,40] The In_2O_3−Au composite, in terms of the threshold sensitivity and output signal, is comparable to the In_2O_3−Pt composite which is a platinum nanoparticle deposited on the anisotropic indium oxide particles.[41]

Comparison of the Output Signals of Our Manufactured and Commercial Sensors. We have reliably determined the lower (threshold) concentrations of acetone at which the electrical resistance of the sensors decreases by about 1.5−1.8 times (by 50−80%). We used the concentration dependencies of the output signals of the sensors for this. These data are compared to similar parameters of commercial sensors (Table 2). Table 2 shows the signal responses of our sensors at 50 ppm of acetone with literature data.

Table 2. Comparison of the Parameters of Our* and Commercial Gas Sensors for the Detection of Acetone Vapors

sensor	platform type	acetone concentration, ppm	output signal, G	output signal G at 50 ppm acetone
MQ 138	Tube	10	1.8	3.3
TGS 822	Tube			4.25
VSP 2110	Planar	2	1.5	5.0
*SnO_2	Planar	1	1.8	6.0
*SnO_2−Au	Planar	0.5	1.7	16
*In_2O_3	Planar	0.1	1.7	32
*In_2O_3−Au	Planar	0.05	2.0	80

It follows from the presented data that the sensors we present in this work are superior in sensitivity in comparison with the available commercial sensors at both low and high acetone concentrations. In the fabrication of commercial sensors, as a rule, SnO_2 is used. These sensors are obtained from $SnCl_4$ and activated with palladium. The size of SnO_2 particles is higher with this method of synthesis (20−35 nm) than those obtained from $SnSO_4$ (4−6 nm). The higher sensitivity of sensors based on SnO_2 developed by us can be explained by both the smaller particle size and the modifying effect of the sulfate groups. The planar type of microheating platforms with an optimal pattern of electrodes and a heating element can also be affected by the value of the output signal. These types of microheating platforms have shown their promise in the production of sensors based on CH_4/CO (ASE-16, ASE-adsorption-sensitive element).

As it is known, modification of the surface of tin dioxide with sulfate groups increases the adsorption capacity of tin cations as Lewis acid centers.[46,47] The strength of acid sites is important for the efficient adsorption of acetone molecules by one of the possible detection mechanisms, in which the acetone molecules adsorption occurs by oxygen of the carbonyl group on metal cations.[12,48] Such a mechanism for detecting acetone makes it possible to explain the higher sensitivity of the samples synthesized by us compared to that of commercial analogues.

Considering the similarity between the detection mechanisms of ethanol and acetone,[46,47] the high sensitivity of indium oxide to acetone can be explained on the basis of the data which are obtained by the detection of ethanol.[49] The effect of the structure and electronic surface states of oxide and gold nanoparticles on the gas sensitivity with respect to ethanol was studied.[24,50,51] Two structural factors determine the gas-sensitive properties of indium oxide. One of them is the ease of changing the indium oxidation state within a significant range without structure restructuring and the occurrence of electronic exchange between them: $In^{2+} - In^{+} + In^{3+}$.[34] The second factor is the presence of indium oxide which is obtained by the sol−gel method of the complex structural defects in the form of oxygen vacancies in interaction with partially reduced states of indium (In^{2+}, In^{+}).[23−33] Such defects are effective centers of adsorption and catalysis, which proceeds according to the associative mechanism through the formation of intermediate complexes from adsorbed molecules and oxygen.[51]

Such a mechanism of adsorption and catalytic oxidation on oxides is characteristic of the molecules of many organic substances.[52−54] Acetone is detected by one of these mechanisms.[5,12] It has been proved by theoretical calculations and experimentally confirmed that initially the coordination of ketone molecules occurs on tin ions by oxygen of the carbonyl group[53,54] followed by a nucleophilic attack of the neighboring hydroxyl group on the carbonyl carbon atom or oxidation with the participation of the active oxygen O^-[48,53]

$$CH_3COCH_3 + O^- \rightarrow CH_3CO^+CH_2 + OH^- + e \quad (1)$$

$$CH_3COCH_3 + OH^- \rightarrow CH_3COO + CH_3O^- \quad (2)$$

It has been shown that oxygen activation in the case of indium oxide is possible on In^{2+} ions in coordination with oxygen vacancies.[26]

Acetone molecules are adsorbed on the surface of Au nanoparticles in the Me_xO_y−Au composites. After that, acetone molecules can react with hydroxyl groups or active oxygen at active sites on the perimeter of the Au particles.[55] A decrease in the electrical resistance of the sensor is recorded at the same time (Figure 8).

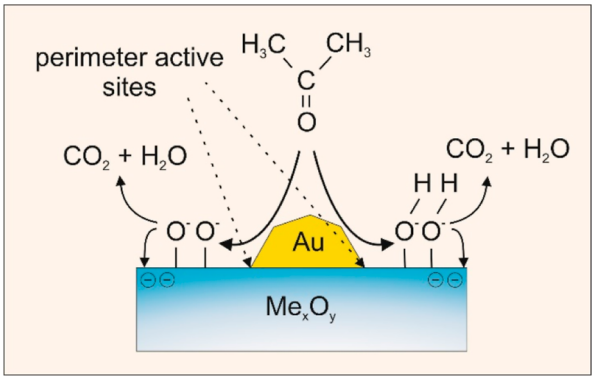

Figure 8. Schematic diagram of acetone oxidation on a Me_xO_y−Au sensor surface.

The increase in sensor sensitivity when adding gold atoms into oxide materials is associated with its participation in the activation of adsorption and catalysis and with its effect on the surface states of the oxide, including on the content of hydroxyl groups.[23] The activity of gold manifests itself upon stabilization in the nanoscale state.[55] The strong binding of Au nanoparticles to the oxide matrix creates sites which are active in

https://doi.org/10.1021/acsomega.3c02125
ACS Omega 2023, 8, 40078−40086

adsorption along the Au/MeO_x perimeter.[23−26] With indium oxide, this interaction of Au nanoparticles with indium oxide is stronger than that with tin dioxide. This is explained by the features of the crystal structure of oxides considered above. Gold clusters on the surface of indium oxide have an electronic bond with indium oxide.[23,25]

CONCLUSIONS

The results of the study showed that sensors based on SnO_2 and In_2O_3 oxides, which have been synthesized by the sol−gel method, have a high sensitivity to low acetone concentrations in a humid environment. The addition of a small amount of Au^{III} ions (0.2 wt %) into tin and indium hydroxide sols increases both the threshold sensitivity and the response of the In_2O_3−Au and SnO_2−Au sensors in the wide range of acetone concentrations. The slope of the calibration curve of In_2O_3−Au-sensors makes it possible to reliably record changes in the acetone concentration in the range of 1.0−5.0 ppm, which is necessary for diagnosing diabetes.

AUTHOR INFORMATION

Corresponding Author

Vladimir Komanicky − *Faculty of Science, Pavol Jozef Šafárik University, Kosice 04001, Slovakia;* orcid.org/0000-0001-8649-1987; Email: vladimir.komanicky@upjs.sk

Authors

Tatiana Kimakova − *Faculty of Medicine, Pavol Jozef Šafárik University, Kosice 04001, Slovakia*

Daria Kondrakhova − *Faculty of Science, Pavol Jozef Šafárik University, Kosice 04001, Slovakia*

Evgeni Ovodok − *Research Institute for Physical-Chemical Problems of the Belarusian State University, Minsk 220030, Belarus*

Marya Ivanovskaya − *Research Institute for Physical-Chemical Problems of the Belarusian State University, Minsk 220030, Belarus*

Valentina Kormosh − *Research Institute of Analytical Technique of Uzhhorod National University, Uzhhorod 88000, Ukraine*

Serhii Vorobiov − *Faculty of Science, Pavol Jozef Šafárik University, Kosice 04001, Slovakia*

Maksym Lisnichuk − *Faculty of Science, Pavol Jozef Šafárik University, Kosice 04001, Slovakia*

Vitalij Bilanych − *Faculty of Science, Pavol Jozef Šafárik University, Kosice 04001, Slovakia; Faculty of Physics, Uzhhorod National University, Uzhhorod 88000, Ukraine*

Complete contact information is available at: https://pubs.acs.org/10.1021/acsomega.3c02125

Notes

The authors declare no competing financial interest.

ACKNOWLEDGMENTS

The work was carried out within the framework of research work 2.1.04.02 SPNI "Chemical Processes, Reagents and Technologies, Bioregulators and Bioorganic Chemistry", 2021−2025; a joint Belarusian-Ukrainian project (grant no. 0121U14006, Ukraine). Work at Safarik University has been supported by the grant of the Slovak Research and Development Agency under contract no. APVV-20-0324 and by the EU NextGenerationEU through the Recovery and Resilience Plan for Slovakia under project no. 09I03-03-V01-00096.

REFERENCES

(1) Hill, D.; Binions, R. Breath Analysis for Medical Diagnosis. *Int. J. Smart Sens. Intell. Syst.* **2012**, *5*, 401−440.

(2) Buszewski, B.; Kesy, M.; Ligor, T.; Amann, A. Human exhaled air analytics: biomarkers of diseases. *Biomed. Chromatogr.* **2007**, *21*, 553−566.

(3) Saasa, V.; Malwela, T.; Beukes, M.; Mokgotho, M.; Liu, C. P.; Mwakikunga, B. Sensing Technologies for Detection of Acetone in Human Breath for Diabetes Diagnosis and Monitoring. *Diagnostics* **2018**, *8* (1), 12.

(4) Righettoni, M.; Tricoli, A. Toward portable breath acetone analysis for diabetes detection. *J. Breath Res.* **2011**, *5* (3), 037109.

(5) Masikini, M.; Chowdhury, M.; Nemraoui, O. Review—Metal Oxides: Application in Exhaled Breath Acetone Chemiresistive Sensors. *J. Electrochem. Soc.* **2020**, *167* (3), 037537.

(6) Wang, D.; Zhang, D.; Yang, Y.; Mi, Q.; Zhang, J.; Yu, L. Multifunctional latex/polytetrafluoroethylene-based triboelectric nanogenerator for self-powered organ-like MXene/metal−organic framework-derived CuO nanohybrid ammonia sensor. *ACS Nano* **2021**, *15*, 2911−2919.

(7) Wang, D.; Zhang, D.; Tang, M.; Zhang, H.; Sun, T.; Yang, C.; Mao, R.; Li, K.; Wang, J. Ethylene chlorotrifluoroethylene/hydrogel-based liquid-solid triboelectric nanogenerator driven self-powered MXene-based sensor system for marine environmental monitoring. *Nano Energy* **2022**, *100*, 107509.

(8) Wang, D.; Zhang, D.; Pan, Q.; Wang, T.; Chen, F. Gas sensing performance of carbon monoxide sensor based on rod-shaped tin diselenide/MOFs derived zinc oxide polyhedron at room temperature. *Sens. Actuators, B* **2022**, *371*, 132481.

(9) Wang, D.; Zhang, D.; Guo, J.; Hu, Y.; Yang, Y.; Sun, T.; Zhan-g, H.; Liu, X. Multifunctional poly (vinyl alcohol)/Ag nanofibers-based triboelectric nanogenerator for self-powered MXene/tungsten oxide nanohybrid NO_2 gas sensor. *Nano Energy* **2021**, *89*, 106410.

(10) Ji, H.; Mi, C.; Yuan, Z.; Liu, Y.; Zhu, H.; Meng, F. Multi-component gas detection method via dynamic temperature modulation measurements based on semiconductor gas sensor. *IEEE Trans. Ind. Electron.* **2023**, *70*, 6395−6404.

(11) Turner, A. P.; Magan, N. Electronic noses and disease diagnostics. *Nat. Rev. Microbiol.* **2004**, *2*, 161−166.

(12) Alizadeh, N.; Jamalabadi, H.; Tavoli, F. Breath Acetone Sensors as Non-invasive Health Monitoring Systems: A Review. *IEEE Sens. J.* **2020**, *20*, 5−31.

(13) Wang, D.; Zhang, D.; Mi, Q. A high-performance room temperature benzene gas sensor based on $CoTiO_3$ covered TiO_2 nanospheres decorated with Pd nanoparticles. *Sens. Actuators, B* **2022**, *350*, 130830.

(14) Liu, Y.; Ji, H.; Yuan, Z.; Meng, F. Conductometric butanone gas sensor based on Co_3O_4 modified SnO_2 hollow spheres with ppb-level detection limit. *Sens. Actuators, B* **2023**, *374*, 132787.

(15) Ji, H.; Liu, Y.; Zhang, R.; Yuan, Z.; Meng, F. Detection and recognition of toluene and butanone in mixture based on SnO_2 sensor via dynamic transient and steady-state response analysis in jump heating voltage mode. *Sens. Actuators, B* **2023**, *376*, 132969.

(16) Ochoa-Muñoz, Y. H.; Mejía de Gutiérrez, R.; Rodríguez-Páez, J. E. Metal Oxide Gas Sensors to Study Acetone Detection Considering Their Potential in the Diagnosis of Diabetes: A Review. *Molecules* **2023**, *28*, 1150.

(17) Ivanovskaya, M. Ceramic and film metaloxide sensors obtained by sol-gel method: structural features and gas-sensitive properties. In *Electron Technology*; Institute of Electron Technology, 2000; Vol. *33*, pp 108−112. https://www.infona.pl/resource/bwmeta1.element.baztech-article-BWA1-0001-0917.

(18) Ovodok, E.; Ivanovskaya, M.; Kotsikau, D.; Kormosh, V.; Alyakshev, I. The structure and the gas sensing properties of nanocrystalline tin dioxide sinthesized from tin (II) sulphate. *Physics, Chemistry and Application of Nanostructures: Reviews and Short Notes to*

https://doi.org/10.1021/acsomega.3c02125
ACS Omega 2023, 8, 40078−40086

Nanomeeting-201.; Borisenko, V. E.; Gaponenko, S. V.; Gurin, V. S.; Kam, C. H., Eds.; World Scientific Publishing: Singapore, 2015; pp 313−316.
(19) Kustov, L. M.; Kazansky, V. B.; Figueras, F.; Tichit, D. Investigation of the acidicproperties of ZrO_2 modified by SO_4^{2-} anions. *J. Catal.* **1994**, *150*, 143−149.
(20) Ovodok, E.; Ivanovskaya, M.; Kotsikau, D.; Kormosh, V.; Pylyp, P.; Bilanych, V. Structural characterization and gas sensing properties of nanosized tin dioxide material synthesized from tin (II) sulfate. *Ukr. J. Phys.* **2021**, *66*, 803.
(21) Gurlo, A.; Ivanovskaya, M.; Pfau, A.; Weimar, U.; Göpel, W. Sol-Gel Prepared In_2O_3 Thin Films. *Thin Solid Films* **1997**, *307*, 288−293.
(22) Vigneron, F.; Caps, V. Evolution in the chemical making of gold oxidation catalysts. *C. R. Chim.* **2016**, *19*, 192−198.
(23) Ivanovskaya, M. I.; Ovodok, E. A.; Kotsikau, D. Sol-gel synthesis and features of the structure of Au-In_2O_3 nanocomposites. *Glass Phys. Chem.* **2011**, *37*, 560−567.
(24) Ivanovskaya, M.; Ovodok, E.; Gaevskaya, T.; Kotsikau, D.; Kormosh, V.; Bilanych, V.; Micusik, M. Effect of Au nanoparticles on the gas sensitivity of nanosized SnO_2. *Mater. Chem. Phys.* **2021**, *258*, 123858.
(25) Ivanovskaya, M. I.; Ovodok, E. A.; Kotikov, D. A. Gas-sensitivity properties of nanoscale Au-In_2O_3 materials. *Russ. J. Gen. Chem.* **2011**, *81*, 2074−2079.
(26) Ivanovskaya, M. I.; Ovodok, E. A.; Kotsikau, D. A. Interaction of carbon monoxide with In_2O_3 and In_2O_3-Au nanocomposite. *J. Appl. Spectrosc.* **2012**, *78*, 842−847.
(27) Malysheva, A. O.; Baldin, M. N.; Gruznov, V. M.; Blinova, L. V. Non-laboratory express gas-chromatographic method of human breath analysis with automated graduation. *Anal. Chem.* **2018**, *22*, 177−185.
(28) Anderson, J. C.; Lamm, W. J. E.; Hlastala, M. P. Measuring airway exchange of endogenous acetone using a single-exhalation breathing maneuver. *J. Appl. Physiol.* **2006**, *100*, 880−889.
(29) Jiang, Z.; Zhao, R.; Sun, B.; Nie, G.; Ji, H.; Lei, J.; Wang, C. Highly sensitive acetone sensor based on Eu-doped SnO_2 electrospun nanofibers. *Ceram. Int.* **2016**, *42*, 15881−15888.
(30) Malysheva, A. O.; Baldin, M. N.; Gruznov, V. M. Determination partition coefficients of volatile organic substances in the system liquid-air for the creation of calibration gas-phase samples with trace concentrations of substances. *J. Anal. Chem.* **2017**, *72*, 1013−1017.
(31) Ioffe, B. F.; Vitenberg, A. G. *Head-Space Analysis and Related Methods in Gas Chromatography*; Leningrad, Khimiia, 1984; Vol. *304*. https://www.wiley.com/en-us/Head+Space+Analysis+and+Related+Methods+in+Gas+Chromatography-p-9780471065074
(32) Mansour, E.; Vishinkin, R.; Rihet, S.; Saliba, W.; Fish, F.; Sarfati, P.; Haick, H. Measurement of Temperature and Relative Humidity in Exhaled Breath. *Sens. Actuators, B* **2020**, *304*, 127371.
(33) Gurlo, A.; Barsan, N.; Weimar, U.; Ivanovskaya, M.; Taurino, A.; Siciliano, P. Polycrystalline well-shaped blocks of indium oxide obtained by the sol-gel method and their gas-sensing properties. *Chem. Mater.* **2003**, *15*, 4377−4383.
(34) De Wit, J. H. W. Structural Aspects and Defect Chemistry in In_2O_3. *J. Solid State Chem.* **1977**, *20*, 143−148.
(35) Cosandey, F.; Madey, T. E. Growth, morphology, interfacial effects and catalytic properties of Au on TiO_2. *Surf. Rev. Lett.* **2001**, *08*, 73−93.
(36) Gu, F.; Di, M.; Han, D.; Hong, S.; Wang, Z. Atomically dispersed Au on In_2O_3 nanosheets for highly sensitive and selective detection of formaldehyde. *ACS Sens.* **2020**, *5*, 2611−2619.
(37) Kotsikau, D.; Ivanovskaya, M.; Ovodok, E.; Azarko, I.; Dakuko, E. State of nanosized Au particles in semiconducting SnO_2 matrix by EPR and UV-VIS spectroscopy. *Int. Meeting "Clusters and nanostructured materials" (CNM-3)*. 2012, Kurdumov Institute of Metal Physics of the NAS of Ukraine, Sept. 30 − Oct. 3. Uzgorod, Ukraine, Uzgorod; Vol. *137*. https://www.nas.gov.ua/EN/Book/Pages/default.aspx?BookID=0000006634.
(38) Zhang, S.; Song, P.; Zhang, J.; Yan, H.; Li, J.; Yang, Z.; Wang, Q. Highly sensitive detection of acetone using mesoporous In_2O_3 nanospheres decorated with Au nanoparticles. *Sens. Actuators, B* **2017**, *242*, 983−993.
(39) Liu, X.; Tian, X.; Jiang, X.; Jiang, L.; Hou, P.; Zhang, S.; Sun, X.; Yang, H.; Cao, R.; Xu, X. Facile preparation of hierarchical Sb-doped In_2O_3 microstructures for acetone detection. *Sens. Actuators, B* **2018**, *270*, 304−311.
(40) Liu, X.; Zhao, K.; Sun, X.; Duan, X.; Zhang, C. X. Xu.; Xu, X. Electrochemical sensor to environmental pollutant of acetone based on Pd loaded on mesoporous In_2O_3 architecture. *Sens. Actuators, B* **2019**, *290*, 217−225.
(41) Liu, W.; Xu, L.; Sheng, K.; Zhou, X.; Dong, B.; Lu, G.; Song, H. A highly sensitive and moisture-resistant gas sensor for diabetes diagnosis with Pt@In_2O_3 nanowires and a molecular sieve for protection. *NPG Asia Mater.* **2018**, *10*, 293−308.
(42) Liu, H.; Qu, F.; Gong, H.; Jiang, H.; Yang, M. Template free synthesis of In_2O_3 nanoparticles and their acetone sensing properties. *Mater. Lett.* **2016**, *182*, 340−343.
(43) Cao, J.; Zhang, N.; Wang, S.; Chen, C.; Zhang, H. Researching the crystal phase effect on gas sensing performance in In_2O_3 nanofibers. *Sens. Actuators, B* **2020**, *305*, 127475.
(44) Che, Y.; Feng, G.; Sun, T.; Xiao, J.; Guo, W.; Song, C. Excellent gas-sensitive properties towards acetone of In_2O_3 nanowires prepared by electrospinning. *Colloid Interface Sci. Commun.* **2021**, *45*, 100508.
(45) Sun, X.; Hao, H.; Ji, H.; Li, X.; Cai, S.; Zheng, C. Nanocasting synthesis of In_2O_3 with appropriate mesostructured ordering and enhanced gas-sensing property. *ACS Appl. Mater. Interfaces* **2014**, *6*, 401−409.
(46) Berger, F.; Beche, E.; Berjoan, R.; Klein, D.; Chambaudet, A. An XPS and FTIR study of SO_2 adsorption on SnO_2 surfaces. *Appl. Surf. Sci.* **1996**, *93*, 9−16.
(47) Babaeva, M. A.; Tsyganenko, A. A.; Filimonov, V. N. IR-spectra of adsorbed SO_2. *Kinet. Catal.* **1984**, *25*, 787.
(48) Abokifa, A. A.; Haddad, K.; Fortner, J.; Lo, C. S.; Biswas, P. Sensing mechanism of ethanol and acetone at room temperature by SnO_2 nano-columns synthesized by aerosol routes: theoretical calculations compared to experimental results. *J. Mater. Chem. A* **2018**, *6*, 2053−2066.
(49) Kohl, D. Surface Processes in the Detection of Reducing Gases with SnO_2-Based Devices. *Sens. Actuators, B* **1989**, *18*, 71−113.
(50) Ivanovskaya, M.; Kotsikau, D.; Faglia, G.; Nelli, P. Influence of chemical composition and structural factors of Fe_2O_3/In_2O_3 sensors on their selectivity and sensitivity to ethanol. *Sens. Actuators, B* **2003**, *96*, 498−503.
(51) Ovodok, E.; Ivanovskaya, M.; Kotsikau, D.; Kormosh, V.; Alyakshev, I.; Muratov, D. Nanostructurized materials based on SnO_2−In_2O_3 for semiconducting sensors to ethanol. *Int. Meeting "Clusters and nanostructured materials" (CNM-3)*, 2012 Kurdumov Institute of Metal Physics of the NAS of Ukraine, Sept. 30 − Oct. 3. Uzgorod, Ukraine. Uzgorod; Vol. *139*. https://www.nas.gov.ua/EN/Book/Pages/default.aspx?BookID=0000006634.
(52) Kiselev, V. F.; Krylov, O. V. *Adsorption and Catalysis on Transition Metals and Their Oxides*; Springer: Berlin, Heidelberg, 1989; pp 136−265..Adsorption and Catalysis on Oxides of Transition Metals
(53) Thoren, W.; Kohl, D.; Heiland, G. Kinetic studies on the decomposition of CH_3COOH and CH_3COOD on SnO_2 single crystals. *Surf. Sci.* **1985**, *162*, 402−410.
(54) Harrison, P. G.; Maunders, B. M. Tin Oxide Surfaces Part 11. Infrared study of the chemisorption of ketones on tin (IV) oxide. *J. Chem. Soc., Faraday Trans. 1* **1984**, *80*, 1329−1340.
(55) Daniel, M. C.; Astruc, D. Gold Nanoparticles: Assembly, Supramolecular Chemistry, Quantum-Size-Related Properties, and Applications toward Biology, Catalysis, and Nanotechnology. *Chem. Rev.* **2004**, *104*, 293−346.

https://doi.org/10.1021/acsomega.3c02125
ACS Omega 2023, 8, 40078−40086